compared with those from simulation software tool [8], and radiation patterns at different frequencies of UWB band are presented.

3. RESULTS AND DISCUSSION

An antenna prototype based on the optimized parameters was fabricated and measured. The antenna return loss was measured with Agilent 8722ES network analyzer, and the radiation patterns were measured over the UWB with a hybrid near-field/far-field antenna measurement system [9], RF-Lab, INRS in Montreal, Canada.

Figure 4 shows the experimental and simulated antenna return loss. From these curves, it can be concluded that the antenna provides a bandwidth from 3 to 10 GHz with a return loss below -10 dB. Two close resonances can be observed, the first one at 4 GHz and the second one around 8 GHz. Current distribution at these frequencies are depicted in Figure 5.

The radiation patterns at different frequencies, namely 4, 7, and 10 GHz, are plotted in Figures 6–8, respectively. The radiation patterns in the H-plane at different frequencies are omnidirectional; they are similar to classical monopole radiation pattern for the H-plane. However, for the E-plane, the radiation patterns vary in the frequency; at lower frequencies, the structure behaves like a dipole, because the curved ground plane and the monopole branch act jointly like dipole arms [Fig. 5(a)]. Around 8 GHz [Fig. 5(b)], the E-plane is identical to monopole, the lower curved side of the structure behaves as a ground plane, and the beams are tilted by 30° with a null at $\theta = 90°$. At higher frequencies, higher modes will interfere and patterns change drastically. With the help of simulation tool, the antenna efficiency has been recorded to be >95% over the entire antenna bandwidth.

4. CONCLUSION

In this article, an UWB antenna has been designed. This monopole-shape antenna uses a third-order binomial law curve for both the monopole branch and the modified ground plane. The antenna has a small size (40×30 mm^2) with a dipole-like radiation pattern for azimuth plane. For elevation plane, the antenna behaves like a dipole at 4 GHz. The monopole and the ground planes act similarly to the branches of this new dipole-like structure. Besides that, at 7 GHz, the current distribution resonates with the monopole edge and hence the structure behaves like a classical monopole. The antenna bandwidth meets UWB requirements.

REFERENCES

1. C.P. Fortier and P.-M. Tardif, Geolocation for UWB networks in underground mines, In: IEEE wireless and microwave technology conference (WAMICON 06), 2007, pp. 1–4.
2. K.L. Wong, Compact and broadband microstrip antennas, Wiley, Hoboken, NJ 2002.
3. R. Chair and A.A. Kishk, Ultra wide-band coplanar waveguide-fed rectangular slot antenna, IEEE Antennas Wireless Propag Lett 3 (2004), 227–229.
4. M. Abbosh and M.E. Bialkowsky, Design of ultrawideband planar monopole antennas of circular and elliptical shape, IEEE Trans Antennas Propag 56 (2008), 17–23.
5. T.A. Denidni and M.A. Habib, Broadband printed CPW-fed circular slot antenna, Electron Lett 42 (2006), 135–136.
6. M.A. Habib and T.A. Denidni, Design of a new wideband microstrip-fed circular slot antenna, Microwave Opt Technol Lett 48 (2006), 919–923.
7. W.L. Stutzman and G.A. Thiele, Antenna theory and design, 2nd ed., Wiley, New York, NY 1998.
8. HFSS v. 11, Ansoft Corp., Pittsburgh, PA.
9. Allwave corp., Available at: http://www.allwavecorp.com, Torrance, California.

COUPLED MICROSTRIP LINE BANDPASS FILTER WITH HARMONIC SUPPRESSION USING RIGHT-ANGLE TRIANGLE GROOVES

Ashraf S. Mohra
Department of Electrical Engineering, College of Engineering, King Saud University, P.O. Box 800, Riyadh 11421, Saudi Arabia;
Corresponding author: amohra@ksu.edu.sa

Received 11 January 2009

ABSTRACT: *A single grooved coupled line bandpass filter with improved pass band response and first harmonic suppression is described. The suppression of the first spurious harmonic was done by using right-angle triangle grooves in the middle of each of the coupled-microstrip lines that construct the bandpass filter. As the number of grooves increase as the shift in the operating frequencies increase also, so it is suitable to use less numbers of grooves as possible. A three stage bandpass filter using coupled-microstrip lines was designed, simulated, and realized to illustrate this idea. The simulated results illustrate a good performance for right-angle triangle groove over the corresponding rectangular groove. The measured S-parameters measurement of the realized bandpass filter shows the suppression of the second resonance frequency and less shift in the center frequency.* © 2009 Wiley Periodicals, Inc. Microwave Opt Technol Lett 51: 2313–2318, 2009; Published online in Wiley InterScience (www.interscience.wiley.com). DOI 10.1002/mop.24644

Key words: *coupled microstrip line; bandpass filter; harmonic suppression; grooves*

1. INTRODUCTION

Coupled-microstrip lines have been widely used in design of bandpass filters due to several attractive features such as compact size, low profile, and tightened capacitive coupling. The bandpass filters based on microstrip-coupled line have been widely used in many microwave systems [1, 2]. The required design parameters of bandpass filter can be easily derived for Butterworth, Chebyshev, or any other prototypes in many literatures [1–3]. However, the microstrip bandpass filter with uniform coupled-microstrip line sections usually suffers from the spurious passband at the second resonant frequency of the microstrip-line resonator. Consequently, it makes the upper stopband performance worse. This problem happened due to the inequality of the even and odd mode velocities of propagation in the inhomogeneous dielectric medium. For a given parallel-coupled-microstrip line structure, the odd mode is propagating faster than the even mode, so the phase constant for the odd mode is less than the corresponding for the even mode; ($\beta_{odd} < \beta_{even}$). In addition, the electromagnetic energy for the odd mode concentrates around the center gap between the coupled lines, whereas for the even mode, the electromagnetic energy concentrates around the metallic edges. Various techniques have been proposed to equalize the even and odd mode velocities or their electrical lengths [4, 5]. Although these techniques lead to the minimization of the harmonics responses, but it need to reconstruct and redesign the filter with new physical design parameters.

In fact, the equal width coupled-microstrip filters suffer from the presence of spurious passband at harmonics of the desired frequency. So, if the conventional parallel-coupled-line filter is used at the next stage of frequency converter in the typical RF communication module, it is very difficult to reject the harmonic signal that frequency converter generates. Consequently, these phenomena result in the degradation of system performance. To lower the rejection level of these harmonics, the low pass filter or

notch filter is connected to the bandpass filter in a series. This solution increases the overall size of RF module and introduces additional insertion losses. Hence, it is necessary to obtain a design technology that can reduce the filter size and reject a harmonic signal.

To reject harmonic signals and reduce the total size, a uniplanar compact photonic bandgap (PBG) structure with periodic patterns etched in the ground plane has been proposed, but the physical and electrical parameters of coupled lines must be recalculated in this structure [6]. Other PBG structures having Blackman, Cosine, Gauss, Hyperbolic Tangent, and Kaiser windows have been proposed by windowing the periodic patterns and the number of periods in the ground plane and using Bragg condition [7–9]. These structures have the increased size problem. Another method to reject the second harmonics by using rectangular grooves is proposed in the literatures [10–13]. The authors use a number of rectangular grooves in all sections, so the second resonance harmonic was suppressed but the designed frequency suffers from shifting to lower value due to the increase in the coupling length of the couplers.

In this article, a right-angle triangle groove is used instead of rectangle groove. The right-angle triangle groove gives better performance than the rectangular groove and at the same times, the frequency shift due to right-angle groove is less than shift due to rectangular groove. Also, it is found that the use of one right-angle triangle groove at the middle of each of the coupled sections is sufficient for the cancellation of the spurious frequency.

2. BANDPASS FILTER DESIGN USING COUPLED-MICROSTRIP LINES

The parallel-coupled-microstrip transmission lines can be used to construct many types of filters. The fabrication of multisection bandpass or bandstop filter coupled line is particularly easy in microstrip or stripline form, for bandwidth less than about 20%. Wider bandwidth bandpass filters generally require very tightly coupled lines. The filter design can be maximally flat (Butterworth) or with ripple value (Chebyshev). In this article, we will use the Chebyshev design. The Chebyshev filter exhibits an equal-ripple response in the passband region and maximally flat response in the stopband region. When the passband ripple is L_{Ar} at the cutoff frequency $\Omega_c = 1$, then the g_n elements for n-element filter are given as follows [2, 14]:

$$g_o = 1.0, \quad g_1 = \frac{2}{\gamma}\sin\left(\frac{\pi}{2n}\right) \tag{1}$$

$$g_i = \frac{1}{g_{(i-1)}} \frac{4\sin\left[\frac{(2i-1)\pi}{2n}\right] \cdot \sin\left[\frac{(2i-3)\pi}{2n}\right]}{\gamma^2 + \sin^2\left[\frac{(i-1)\pi}{n}\right]}, \quad i = 2,3,..N \tag{2}$$

$$g_{i+1} = \begin{cases} 1.0 & \text{for n odd} \\ \coth^2(\beta/4) & \text{for n even} \end{cases} \tag{3}$$

TABLE 1 The Design Data for the Bandpass Filter

N	g_n	Z_{oe} (Ω)	Z_{oo} (Ω)	W (mm)	S (mm)	L (mm)
1	1.5963	70.6047	39.24	3.842	0.283	26.69
2	1.0967	56.64	44.77	4.695	1.592	26.31
3	1.5963	56.64	44.77	4.695	1.592	26.31
4	1.0000	70.6047	39.24	3.842	0.283	26.69

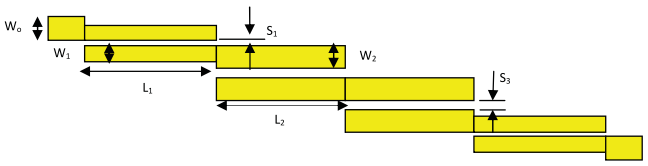

Figure 1 The schematic of the three section bandpass filter using microstrip coupled lines. [Color figure can be viewed in the online issue, which is available at www.interscience.wiley.com]

where

$$\beta = \ln\left[\coth\left(\frac{L_{Ar}}{17.37}\right)\right] \text{ and } \gamma = \sinh\left(\frac{\beta}{2n}\right) \tag{4}$$

where L_{Ar} is the passband ripple (dB). The even-mode and odd-mode impedances (Z_{oe}, Z_{oo}) for the coupled-microstrip lines can be calculated as follows [2]:

$$Z_{oe_x} = Z_o[1 + J_xZ_o + (J_xZ_o)^2] \tag{5a}$$

$$Z_{oo_x} = Z_o[1 - J_xZ_o + (J_xZ_o)^2] \tag{5b}$$

where

$$J_1Z_o = \sqrt{\frac{\pi\Delta}{2g_1}}, \quad J_nZ_o = \frac{\pi\Delta}{2\sqrt{g_n \cdot g_{n-1}}} \quad n = 2,3,\ldots N, \tag{6a}$$

$$J_{n+1}Z_o = \sqrt{\frac{\pi\Delta}{2g_n \cdot g_{n+1}}} \tag{6b}$$

where (Δ) is the fractional bandwidth of the bandpass filter. As an example, a bandpass filter with three-section ($n = 3$) and 0.5 dB equal ripple response was designed at center frequency of 2 GHz, with fractional bandwidth (Δ) of 0.1 on RT/Duroid ($\varepsilon_r = 2.2$, $h = 1.5748$ mm). With the use of above design equations, the parameters of bandpass filters will be as given in Table 1. Figure 1 illustrates the configurations of the design bandpass filters, where Z_o is the terminated characteristic impedance which is 50 ohm, W, S, and L are width, separation, and coupling length of the coupled-microstrip line for each of the coupling sections of the bandpass filter.

3. SIMULATIONS OF BANDPASS FILTER WITH GROOVES

At first, the designed bandpass filter without grooves is simulated on IE3D software package [15] and the simulated results are shown in Figure 2. It appears that the conventional coupled microstrip line bandpass filter generates high signal level at the second harmonic. It appears also, there is a transmission zero (f^o) at 4.4GHz and first harmonic frequency (f^h) at 4.05 GHz. To cancel the effect of second harmonics, the transmission zero must cancelled by first harmonic frequency. The way to make cancellation is done by grooves in the middle of the coupled-microstrip line.

3.1. Bandpass Filter With One Groove

Different simulations were done for the previously designed coupled-microstrip line bandpass filter for each of rectangular groove and right-angle triangular groove with different groove widths and heights, Figure 3. Figure 4 illustrates the effect of different rectangular (R) and right-angle triangular (T) groove heights for

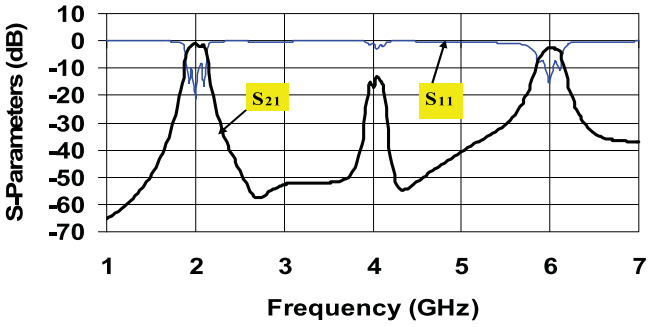

Figure 2 The S-Parameters for Bandpass filter without grooves. [Color figure can be viewed in the online issue, which is available at www.interscience.wiley.com]

constant groove width ($W/4$), where W is the width of the coupled-microstrip section. It appears that the bandpass filter with right-angle triangle groove gives good cancellation for the second harmonics than rectangle groove. It appears also that there is a shift in the operating frequencies to lower value especially for the bandpass filter using rectangular grooves. Figure 5 illustrates the insertion loss of the bandpass filter with groove width = $W/2$ at different groove heights. The bandpass filter with right-angle triangle groove gives good second harmonics cancellation at groove height $W/2$, $3W/4$, whereas the rectangle groove gave better effect at groove height $W/4$ only. Figure 6 illustrates the insertion loss for the bandpass filter with groove width = $3W/4$ at different groove heights. As the groove width increases as the cancellations of the second harmonics decreases, Figure 6, but the right-angle triangle groove still gives better performance than the rectangle grooves.

From the previous discussion the bandpass filter using right-angle triangle groove gives better second harmonics cancellation rather than the use of rectangle grooves especially when groove width equal to groove heights equal to $W/2$. Also, when the groove height is equal to $W/2$, a good performance for the second harmonic cancellation is happened. The grooves width has an effect only on the shift of the operating frequencies for both of the first and third resonance frequencies due to the increase of the coupling length of the coupled-microstrip lines.

The transmission zero (f^o) and first harmonic frequency (f^h) are plotted versus the ratios of grooves height to coupled line width ($H_{Groove}/W_{Coupled\ line}$) at different groove widths, Figure 7. Form this figure, as the ($H_{Groove}/W_{Coupled\ line}$) increase as the cancellation happened at lowest frequency. Also, as the groove width increase as the cancellation happened at larger ($H_{Groove}/W_{Coupled\ line}$) ratio.

The coupled-microstrip line bandpass filter using grooves suffers from the shift of the operating frequencies (first, third, etc.). Figure 8 illustrates the frequency shift for each of rectangular and right-angle triangle grooves ($W_{Groove} = H_{Groove} = W/2$). With referring to Figure 8, the right-angle triangle groove has 25 MHz

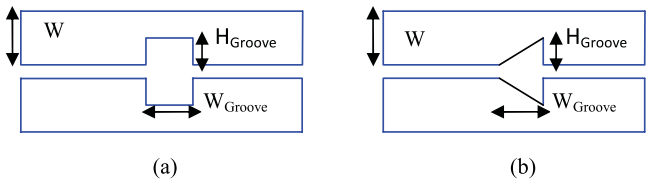

Figure 3 The groove dimensions referred to microstrip couple line width (a) Rectangular groove (b) Right-angle triangle groove. [Color figure can be viewed in the online issue, which is available at www.interscience.wiley.com]

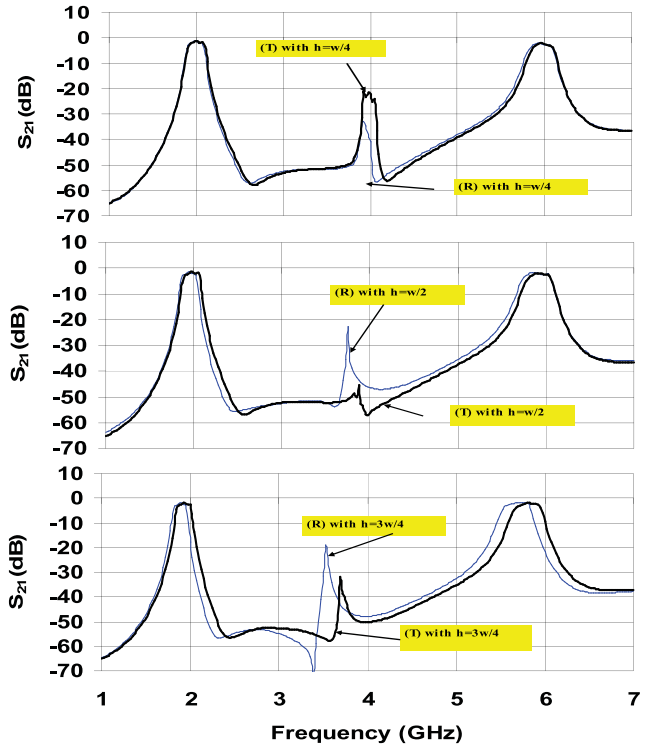

Figure 4 The insertion loss for bandpass filter with rectangular (R) and right-angle Triangle (T) grooves with groove width = W/4 and different groove heights. [Color figure can be viewed in the online issue, which is available at www.interscience.wiley.com]

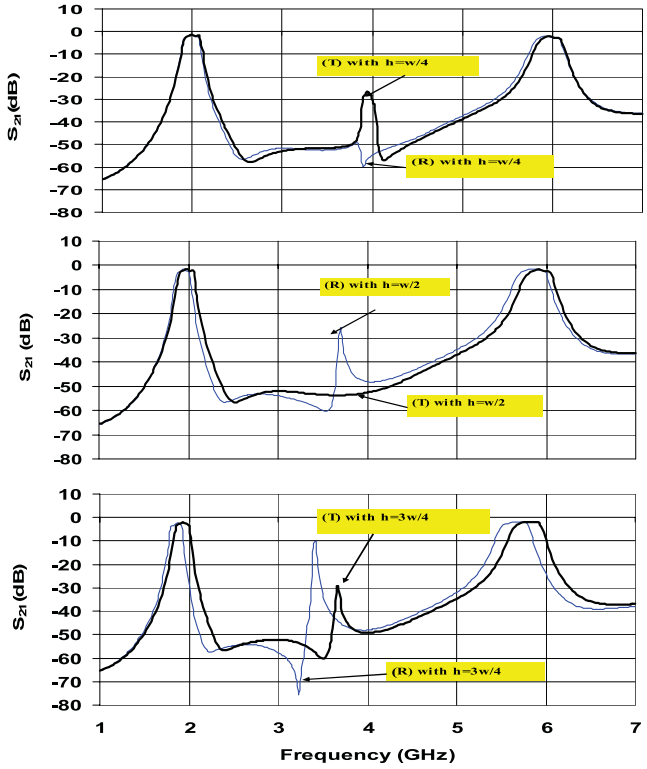

Figure 5 The insertion loss for bandpass filter with rectangular (R) and right-angle triangle (T) grooves with groove width = W/2 at different groove heights. [Color figure can be viewed in the online issue, which is available at www.interscience.wiley.com]

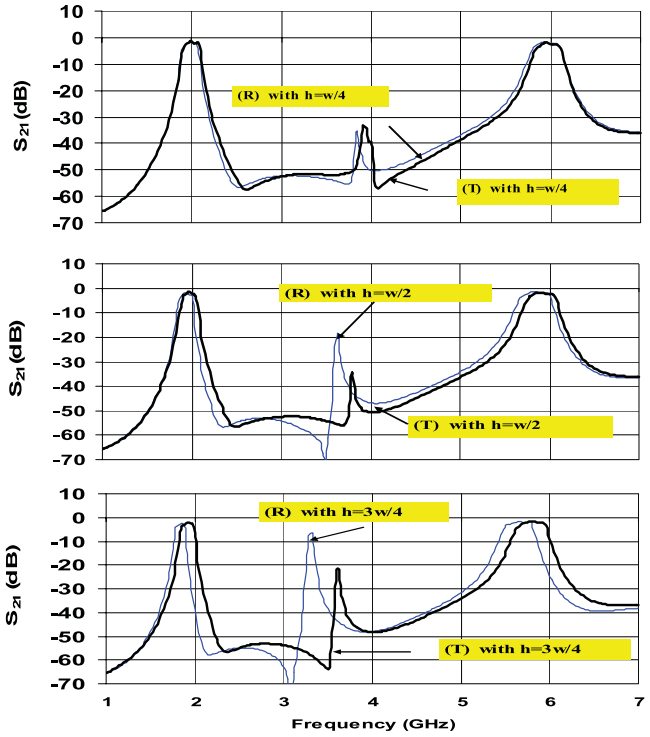

Figure 6 The insertion loss for bandpass filter with rectangular (R) and right-angle Triangle (T) grooves with groove width = 3W/4 at different heights. [Color figure can be viewed in the online issue, which is available at www.interscience.wiley.com]

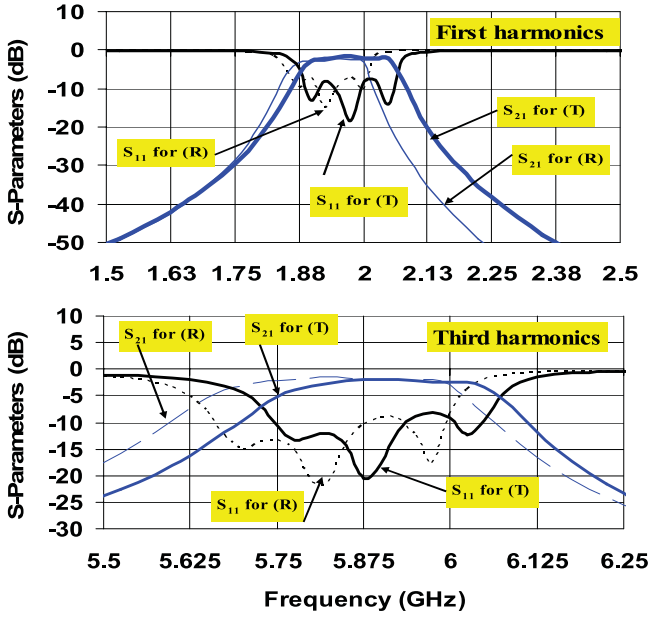

Figure 8 The shift in first and third harmonics for bandpass filter for rectangular (R) and Right-angle triangle grooves. [Color figure can be viewed in the online issue, which is available at www.interscience.wiley.com]

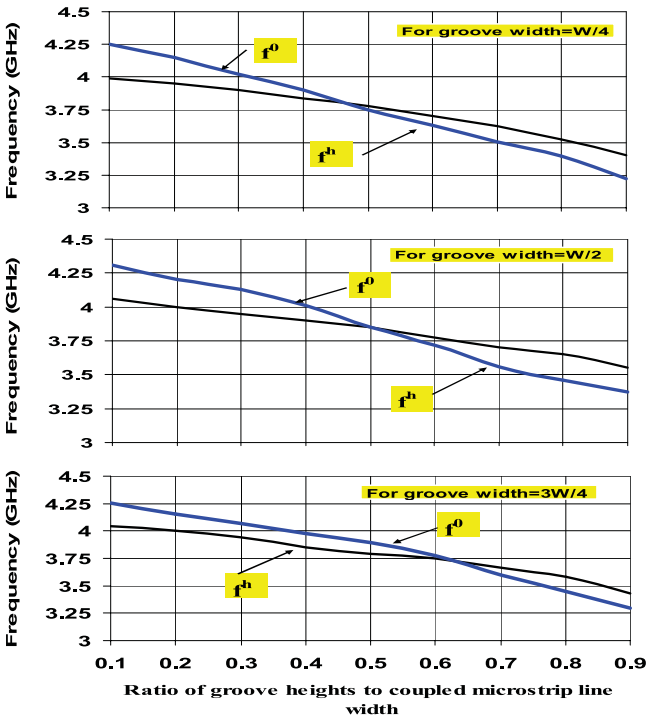

Figure 7 The variations of (f^0) and (f^h) frequencies versus the ratio of groove height to coupled microstrip line width for right-angle triangle grooves. [Color figure can be viewed in the online issue, which is available at www.interscience.wiley.com]

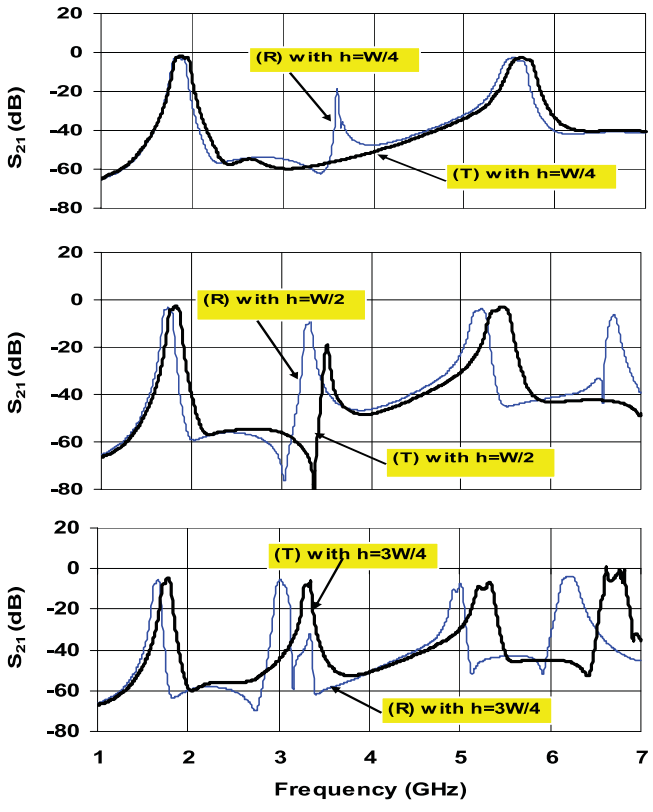

Figure 9 The insertion loss for rectangular (T) and right-angle Triangle (T) groove with groove width = W/4 at different groove heights. [Color figure can be viewed in the online issue, which is available at www.interscience.wiley.com]

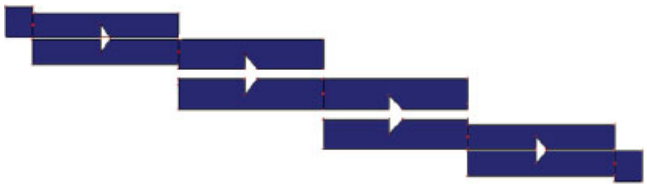

Figure 10 The configuration of the realized bandpass filter. [Color figure can be viewed in the online issue, which is available at www.interscience.wiley.com]

shift for first frequency, whereas the shift is 75 MHz for rectangular grooves. The shift in third frequency for right-angle triangle groove is 125 MHz, whereas it is 200 MHz for rectangular groove. So the right-angle triangle groove gives a less frequency shift than the rectangular groove with the same width and heights.

3.2. Bandpass Filter With Five Grooves

The simulation result for a bandpass filter with five groove is shown in Figure 9 for both of rectangular (R) and right-angle triangle (T) grooves, where all the grooves width ($W/4$) at different heights ($H_{\text{Groove}} = W/4, W/2, 3W/4$). It is clear that as the number of grooves increases as the shift in the operating frequencies increases also. It is appears also, the right-angle triangle groove still gives better performance than the rectangular grooves especially for lower grooves height ($W/4$) and the shift in frequency is less also. Both types of grooves suffer from the presence of spurious harmonic at higher groove heights. By comparing Figures 4 and 9, it is appear that the insertion loss for five right-angle triangle grooves is better by (-5 dB) only than using one right-angle triangle groove for the cancellation of the spurious frequency. Also, the shift in operating frequencies (2 and 6 GHz) for one groove is less than of five grooves. So, the use of one right-angle triangle groove is sufficient for the cancellation of the spurious frequency and giving less frequency shift. To increase the number of grooves, the groove width must be small; otherwise, the operating passband required will damage and a larger shift in the operating frequencies will happened.

4. FABRICATION AND MEASUREMENTS

The designed bandpass filter with one right-angle groove ($W_{\text{Groove}} = H_{\text{Groove}} = W/2$) at the middle of each of the coupled section was realized using microstrip technology and then measured by using Vector Network Analyzer. Figure 10 illustrates the shape of the realized bandpass filter. The comparison between the simulated and measured results is shown in Figure 11, good agreement between simulated and measured results are appear. Figure 12 illustrates the measured insertion loss for bandpass filter without grooves, with rectangular grooves and with right-angle triangle grooves ($W_{\text{Groove}} = H_{\text{Groove}} = W/2$). From the figure, the bandpass filter with right-angle triangle groove gives the better performance. The measured frequency shift for the first and the third operating passband are shown in Figure 13. The bandpass filter that using right-angle triangle grooves have a frequency shift of 16 and 48 MHz for first and third passband (2 and 6 GHz), respectively. The corresponding frequency shift when using rectangular grooves is

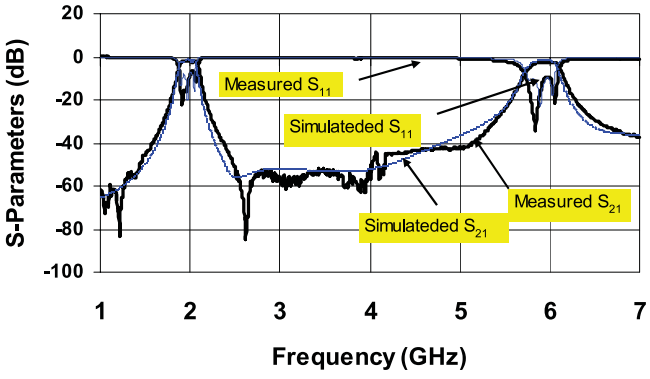

Figure 11 The Simulated and measured S-parameters for BPF with Right-angle Triangle grooves. [Color figure can be viewed in the online issue, which is available at www.interscience.wiley.com]

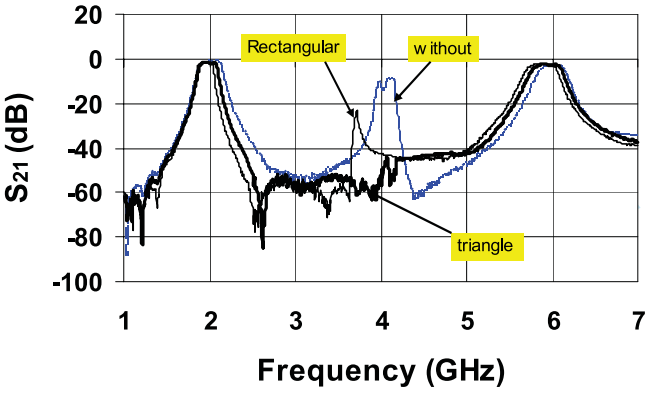

Figure 12 The measured insertion loss for BPF using without, rectangular and right-angle triangle grooves. [Color figure can be viewed in the online issue, which is available at www.interscience.wiley.com]

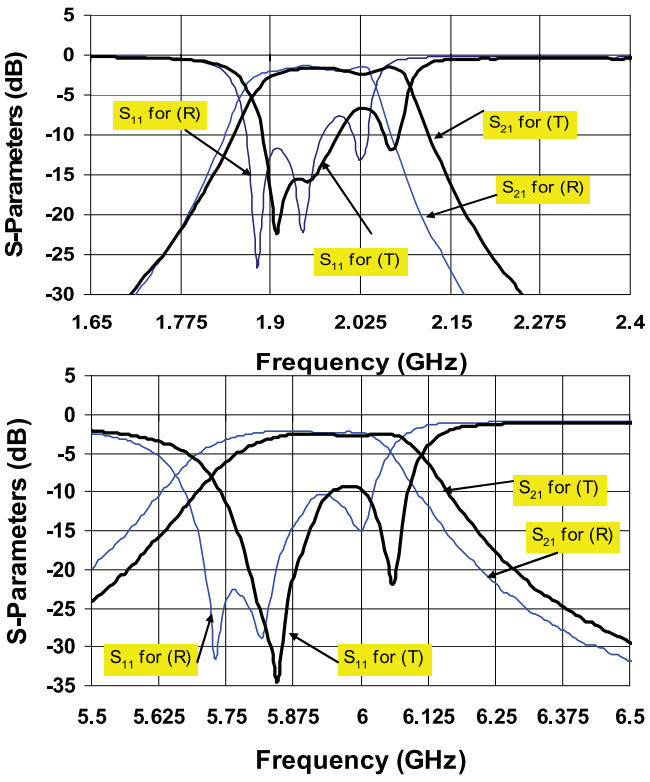

Figure 13 The Measured frequency shift for the first and second operating frequency for of BPF with rectangular and right-angle triangle grooves. [Color figure can be viewed in the online issue, which is available at www.interscience.wiley.com]

80 MHz and 145 MHz. So, the bandpass filter using right-angle triangle grooves is better in frequency shift.

5. CONCLUSIONS

The coupled-microstrip line bandpass filters suffer from the presence of the second harmonics. To cancel the second harmonic, a right-angle triangle groove was used at the center of each of the microstrip-coupled lines. A different grooves width and heights are simulated and compared with the rectangular grooves. The right-angle triangle groove gives better performance and good cancellation for the second harmonic rather than the corresponding rectangular groove. The frequency shift in the operating frequencies when using right-angle triangle grooves is less than that of the rectangular grooves. The measurements of the realized bandpass filter gave good agreement with the simulated results and better results when compared with bandpass filter with rectangular grooves.

ACKNOWLEDGMENTS

The author of this article would like to acknowledge the assistance and financial support provided by Research Center in the College of Engineering at King Saud University.

REFERENCES

1. D. Pozar, Microwave engineering, 3rd ed., Wiley, New York, 2005.
2. J.S. Hong and M.J. Lancaster, Microstrip filters for RF/microwave applications, Wiley, New York, 2001.
3. G. Matthaei, L.F. Young, and R.M.T. Jones, Microwave filters, impedance matching networks and coupling structures, Artech, Boston, MA, 1980.
4. C.-Y. Chang and T. Itoh, Modified parallel couple filter structures that improve the upper stopband rejection and response symmetry, IEEE Trans Microwave Theory Tech 39 (1991), 310–314.
5. B. Ester and K.A. Merze, Parallel couple line filters for inverted microstrip and suspended substrates MICs, 11th European Microwave Conference Digest, 1981, pp. 164–167.
6. F.R. Yang, K.P. Ma, Y. Qian, and T. Itoh, Analysis and application of coupled microstrips on periodically patterned ground plane, IEEE MTT-S Dig, Boston, MA (2000), 1529–1531.
7. J.-T. Kuo, W.-H. Hsu, and W.-T. Huang, Parallel coupled microstrip filters with suppression of harmonic response, IEEE Microwave Wireless Compon Lett 12 (2002), 383–385.
8. M.A.G. Laso, M.J. Erro, T. Lopetegi, D. Benito, M.J. Garde, and M. Sorolla, Optimization of tapered bragg reflectors in microstrip technology, Int J Infrared Millimet Waves 21 (2000), 231–245.
9. T. Lopetegi, M.A.G. Laso, M.J. Erro, D. Benito, M.J. Garde, F. Fal-cone, and M. Sorolla, Novel photonic bandgap microstrip structures using network topology, Microwave Opt Technol Lett 25 (2000), 33–36.
10. B.S. Kim, J.W. Lee, and M.S. Song, An implementation of harmonic suppression microstrip filters with periodic groves, IEEE Microwave Wireless Compon Lett 14 (2004), 413–415.
11. J. Marimuthu and M. Esa, Second harmonic suppression characteristic of a grooved band pass filter, Asia Pacific Conference on Applied Electromagnetic Proceeding, Johor Bahru, Malaysia, 2005, pp. 227–231.
12. S. Sun and L. Zhu, Periodically nonuniform coupled microstrip line filters with harmonic suppression using transmission zero reallocations, IEEE Trans Microwave Theory Tech 53 (2005), 1817–1822.
13. J. Marimuthu and M. Esa, Wideband and harmonic suppression method of parallel coupled microstrip bandpass filter using centered single groove, Proceeding of the 2007 International Conference on Telecommunications Penang, Malaysia, 2007, pp. 622–626.
14. A.S. Mohra and M. Al-Kanhal, Small size stepped impedance low pass filters, Microwave Optical Technol Lett 49 (2007), 2398–2403.
15. IE3D software package, Zeland Company, version 11.00

A FULLY INTEGRATED ULTRA-LOW POWER CMOS TRANSMITTER MODULE FOR UWB SYSTEMS

Tao Yuan,[1,2] Yuanjin Zheng,[2] Le-Wei Li,[1] and Mook-Seng Leong[1]

[1] Department of Electrical and Computer Engineering, National University of Singapore, 4 Engineering Drive 3, Singapore 117576; Corresponding author: yuantao_xd@hotmail.com

[2] Institute of Microelectronics, Agency for Science, Technology and Research, 1 Fusionopolis Way, Singapore 138632

Received 21 January 2009

ABSTRACT: *A fully integrated CMOS ultra-wideband (UWB) transmitter module is proposed for UWB applications. The transmitter module consists of a band-notched UWB antenna and a transmitter IC which integrates a pulse generator, a gating signal generator and driver amplifiers (DAs). The drive amplifier uses a two-stage amplifier—a Class-E amplifier and a Class-A amplifier with switch control, to significantly reduce power consumption (522 μW/20 Mbps). Fabricated using a 0.18-μm CMOS process, the generated pulse then passes through the DA, which not only drives the antenna but also shapes the generated digital signal to meet the Federal Communications Commission spectral mask specification.* © 2009 Wiley Periodicals, Inc. Microwave Opt Technol Lett 51: 2318–2323, 2009; Published online in Wiley InterScience (www.interscience.wiley.com). DOI 10.1002/mop.24632

Key words: *ultra-wideband (UWB); pulse generators; amplifier; CMOS transmitter; antennas*

1. INTRODUCTION

The ultra-wideband (UWB) technology has received considerable attention because the US Federal Communications Commission (FCC) released an unlicensed spectrum of 3.1–10.6 GHz for commercial wireless applications. UWB systems have many advantages over traditional narrowband wireless systems, such as noise/interference immunity, low probability of undesired detection, interception, implementation with low cost and low-power consumption, high-data rates, and coexistence with other wireless communication systems [1]. In impulse UWB systems, the pulse generator is a key component for both the transmitter and receiver [2]. The complex pulse shaping network can be achieved by using a dedicated circuit that consumes very little power [3, 4]. To reduce the power consumption which is proportional to the data rate, direct pulse generation is feasible in impulse radio communication of 3.1–10.6 GHz UWB band. It possesses the favored characteristics of low cost and low power because it is realizable by digital CMOS technologies [5–7].

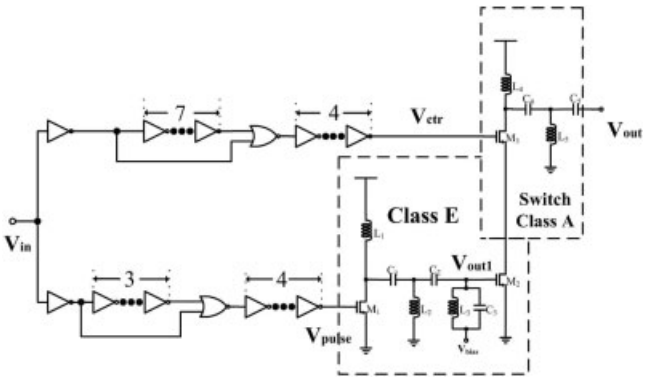

Figure 1 Circuit design of the UWB transmitter IC